Development and testing of the gravitational wave antenna MiniGRAIL in its full-featured configuration

Usenko, O.

Chapter 2

MiniGRAIL data acquisition system

Introduction

In the previous chapter we have shown that for full omnidirectional operation of MiniGRAIL a simultaneous data from 6 transducers has to be acquired. In the current chapter we describe the acquisition system that was developed for a full featured MiniGRAIL operation.

We have set up the 8-channel acquisition system using a PC with 24-bit National Instruments NI 4472-PCI analog-digital converter(ADC) card. The acquired data is saved over the network to a 4TB RAID5 storage system. A GPS clock is used for precise timing of the acquisition.
The acquisition libraries are written in c/c++ and user interface modules are written in c#. Software to monitor the the dilution refrigerator operation and less important auxiliary acquisition modules are made in LabView [41]. The preprocessing of the acquired data is done in Matlab [34]. The full data processing pipeline is being developed by a group in the university of Geneva[31]. We have also developed scripts that allow the synchronization of the acquired data with the university of Geneva.

A summary of key acquisition system parameters is given below:

- 6 capacitive transducers, read out by 6 double stage SQUIDs are installed on the sphere for omnidirectional data analysis.
- SQUIDS are controlled by commercial 8-channel SQUID electronics [42]
- 24 bit 8 channel analog-digital converter (NI 4472-PCI)(one channel is reserved for GPS timing) is used to digitize the data.
- Timing is done with a GPS system: Trimble Accutime 2000 ($\pm 25\, ppm$ accuracy)
- Acquisition frequency: $\approx 20\, kHz$

- Data rate is 80 KB/s ($\approx 275\,MB/h$) per channel

If we are doing a full seven channel acquisition, the amount of data acquired per day is approximately $45\,GB$. This would probably not impress the high energy physicists and astronomers, but for a laboratory scale experiment it is not usual. We have set up a $4\,TB$ RAID5 NAS (Network Attached Storage) to store the data. With the current capacity it is enough to store about 3 months of MiniGRAIL data.

To maintain the stability of the main (fast) acquisition system we do not perform any tasks on the acquisition PC, but we have set up a second acquisition PC with a 16-bit National Instruments NI PCI-6034E ADC card which used to monitor the SQUIDs noise and working point and for calibration purposes.

Since cosmic rays can also excite the MiniGRAIL sphere, a cosmic ray detector, which is a part of HiSparc [43] project, is installed on the laboratory roof above MiniGRAIL. The data from the detector is also recorded with precise GPS timing and can be combined with MiniGRAIL data for vetoing the cosmic rays events. As we already know, the unique property of MiniGRAIL is that unlike the bar detectors, the spherical detector reacts differently to the gravitational waves and cosmic rays, so it is possible to distinguish these perturbation by looking at different sphere modes [15].

2.1 Data acquisition

2.1.1 Hardware

The general scheme of the acquisition system is shown on fig. 2.1 To improve the reliability the acquisition system is split into few independent parts each of them running on separate PC's

Further in this chapter we will take a closer look at each component of the system.

SQUID amplifier

Even amplified by the resonant transducer, the signal coming from the sphere is very weak. This puts very high requirements on the amplifiers we need to use. It should have very low intrinsic noise and be placed as close to the transducer as possible. A dc SQUID amplifier is likely an ideal solution - it is one of the most sensitive magnetic flux-to-voltage converters and it works the best at ultracryogenic temperatures. Operation principle and design of the dc SQUIDs are widely described in literature, so we will only give here a short introduction.

SQUID operation is based on the effect of tunnelling of Cooper pairs through an insulating barrier (a junction) between two superconductors, which was predicted by B. Josephson in 1962 [44]. Josephson showed that the current I flowing through a junction is given by

$$I = I_0 \sin(\delta) \tag{2.1}$$

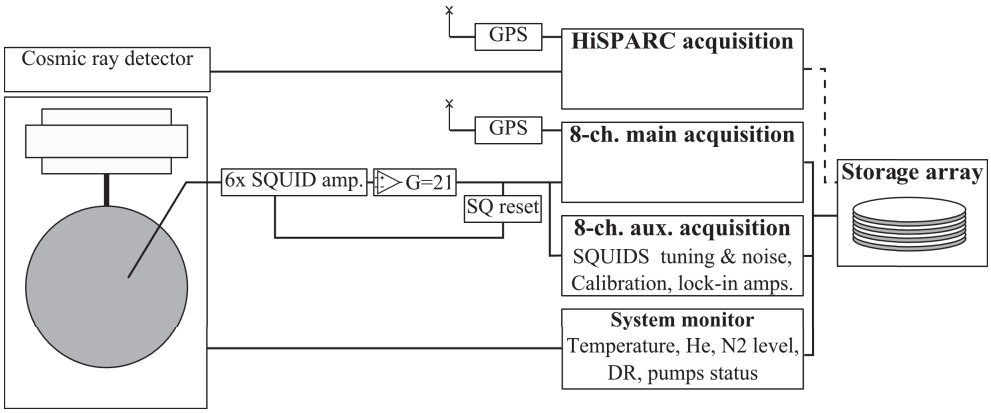

Figure 2.1**:** Acquisition system of MiniGRAIL. Besides the main acquisition system which is used to digitize and store the signal from 6 transducers we have set up an auxiliary acquisition used to do the SQUIDS monitoring and calibration without disturbing the main system. A separate PC is used to monitor system parameters like temperature, dilution refrigerator operation, etc. The data of MiniGRAIL and HiSparc can be synchronized by using a GPS timing

where $\delta = \phi_1 - \phi_2$ is the difference between the phases ϕ_1 and ϕ_2 of the condensates in the two superconducting electrodes and I_0 is the maximal supercurrent (critical current) through a junction. If a voltage V is applied between the superconducting electrodes, the phase difference evolves in time as

$$\frac{d\delta}{dt} = \frac{2\pi}{\Phi_0} V = 2\pi f_J, \tag{2.2}$$

where $\phi_0 = h/2e = 2.07 \times 10^{-15}$ Wb is the magnetic flux quantum and $f_J = \frac{V}{\Phi_0} = 483 \frac{MHz}{\mu V} V$ is called the Josephson frequency. From equations (2.1) and (2.2) we see that in zero voltage state the phase difference is constant in time and the current through the junction can not exceed I_0. If $V > 0$ the current starts oscillating with the Josephson frequency. A high-quality tunnel junction has a hysteretic current-voltage characteristics. As the current through the junction (a bias current) is increased from zero, the voltage switches to a non-zero value when I_b exceeds I_0, but returns to zero only when the current is reduced to a value much less than I_0. This hysteresis can be eliminated by shunting the junction with an external shunt resistance. The current-voltage characteristics of such junctions is well explained by the resistively- and capacitively-shunted junction (RCSJ) model [45].

A SQUID amplifier consists of two Josephson junctions connected in parallel and forming a superconducting loop. A schematic of a dc SQUID is shown on figure 2.2. A junction is conventionally represented on schemes with a cross symbol. An insulating barrier between the superconductors forms a capacitance C parallel to the junction.

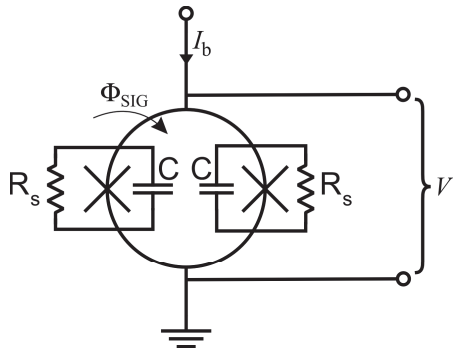

Figure 2.2**:** Scheme of a dc SQUID. The crosses represent the Josephson junctions of capacitance C. Shunt resistors R_s across the junctions are used to remove hysteresis.

Shunt resistor R_s are added to remove the junction hysteresis. The hysteretic behaviour of the junction is characterized by McCumber parameter $\beta_c = \omega_J R_s C$. If $\beta_c < 1$, the I-V characteristic of the Josephson junction is non-hysteretic and if $\beta_c > 1$, the junction shows hysteretic behavior. For the SQUIDs we use, β_c is always less then one.

The change of flux through the SQUID loop modulates its critical current with a period of Φ_0. The two extremal I-V curves are shown on figure 2.3(a). The modulation depth of the critical current is given by

$$\Delta I_c \approx \frac{1}{1+\beta_L} 2I_0, \tag{2.3}$$

where the screening parameter β_L is

$$\beta_L = \frac{2I_0 L_{SQ}}{\Phi_0} \sim 1. \tag{2.4}$$

If we bias a SQUID with a constant current $I_b > 2I_0$, the resulting voltage V across a dc SQUID will be a periodic function of external magnetic flux Φ_{sig} as shown on figure 2.3(b).

The maximum gain of the SQUID $V_{\Phi_{max}}$ is estimated as

$$V_{\Phi_{max}} \equiv \frac{\partial V_{max}}{\partial \Phi} = \frac{2\beta_L}{1+\beta_L} \frac{R}{L_{SQ}}. \tag{2.5}$$

Noise of a SQUID amplifier

In chapter 1 we have already introduced the noise of a SQUID amplifier. Its origin is the Johnson noise of the shunt resistor given as

$$S_V(\omega) = 4k_B T R_s \tag{2.6}$$

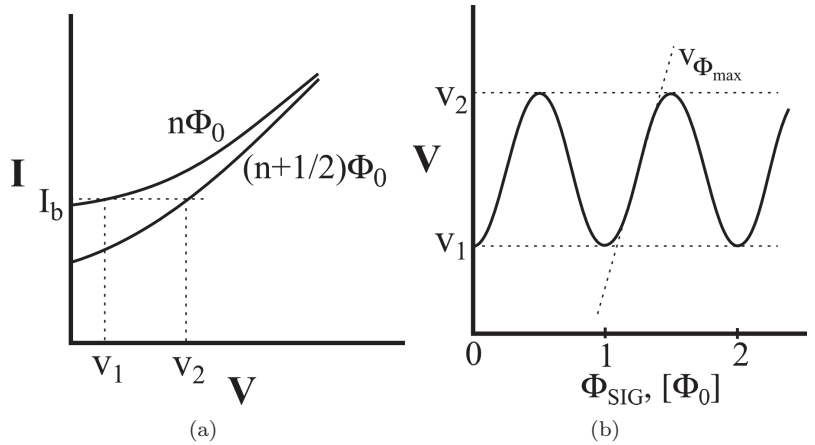

Figure 2.3**:** $I-V$(a) and $V-\Phi$(b) characteristics of a dc SQUID.

The spectral density of a voltage noise at the output of a dc SQUID is given by

$$S_{VV} = \gamma 2 S_I {R_{dyn}}^2 \sim \gamma_{VV} k_B T R_s, \tag{2.7}$$

where $R_{dyn} \sim R_s/2$ is the dynamic resistance of the SQUID. The resistors also generate a circulating current noise in the SQUID that induces noise into any input circuit coupled to it. Its spectral density is given by

$$S_{JJ} = \gamma_{JJ} \frac{k_B T}{R_s}. \tag{2.8}$$

A cross correlation between voltage and current noise contributes as well to the total noise in the SQUID with a spectral density of

$$S_{JV} = \gamma_{JV} k_B T. \tag{2.9}$$

The coefficients $\gamma_{VV}, \gamma_{JJ}, \gamma_{JV}$ arise from the fact that Johnson noise is generated at frequencies around the Josephson frequency f_J is mixed down to the measurement frequency by the Josephson oscillations and the inherent non-linearity of the junctions. These can be numerically evaluated as $\gamma_{VV} \sim 16$, $\gamma_{JJ} \sim 11$, $\gamma_{JV} \sim 12$ [26].

For uncoupled SQUID only the the S_{VV} term gives noticeable contribution to the noise. If the SQUID is connected to the input circuit, both current and voltage terms couple back to the input coil as described in equation (1.34) of section 1.2.2.

Using equation (2.5) and equation (2.7), the flux noise spectral density at the input of the SQUID can be calculated as

$$S_\Phi = \frac{S_{VV}}{V_{\Phi_{max}}^2} \sim \gamma_{VV} \frac{k_B T {L_{sq}}^2}{R_s} \left(\frac{1+\beta_L}{2\beta_L}\right)^2. \tag{2.10}$$

This equation is valid for $\beta_L \sim 1$.

A convenient way to compare the sensitivity of different SQUIDs is in terms of the noise energy per unit bandwidth or energy resolution:

$$\epsilon = \frac{S_\Phi}{2L_{sq}} = \gamma_{VV}\frac{k_B T L_{sq}}{2R_s}\left(\frac{1+\beta_L}{2\beta_L}\right)^2 \tag{2.11}$$

According to equation (2.11), the energy resolution can be improved by decreasing the SQUID inductance L_{sq} and/or the operating temperature T. The limit in decreasing L_{sq} is given by the increasing of the impedance mismatch to a conventional signal source, which might have a few μH of internal inductance. Moreover, the intrinsic energy sensitivity of a dc SQUID is inversely proportional to the critical current density of the junctions if the parameters β_L and β_C are about 1. When $\beta_L \sim 1$, the energy resolution becomes $\epsilon = \gamma_{VV} k_B T \Phi_0 / 4R_s I_0$. This means that increasing the critical current, while keeping $\beta_L, \beta_C \sim 1$ is another procedure to minimize the dc SQUID intrinsic noise [46].

SQUID readout

While being one of the most sensitive magnetic flux-to voltage converters, the SQUID amplifiers do not have a very high gain. Given typical parameters of resistively shunted dc SQUID, the resulting flux to voltage transfer is of the order of $\frac{\partial V}{\partial \Phi} = 100\,\mu V/\Phi_0$ and the voltage swing is $2\delta V = V_1 - V_2 \sim 30\,\mu V$. The wideband flux noise of the dc SQUID is typically around $1 - 2\mu\Phi_0/\sqrt{Hz}$. This corresponds to an output voltage noise of $0.1\,nV/\sqrt{Hz}$, which is about one order of magnitude smaller than the input voltage noise of typical low-noise room temperature preamplifiers. This problem can be solved by using a two stage SQUID system, when a second SQUID amplifies the sensor dc SQUID [47]. A scheme of 2-stage SQUID amplifier with a readout electronics is shown on figure 2.4.

Let us first look at the 2-stage SQUID configuration. A first (sensor) SQUID is biased at a constant voltage by sending a bias current I_{b1} through a small resistance $R_b \ll R_{dyn1}$ in parallel to the SQUID. In this mode, the SQUID acts as a flux-to-current converter, so the signal flux generated by current I_1 in the input coil is converted to a current I_2 in the input coil of the second (amplifier) SQUID. The flux gain G_Φ of 2-stage SQUID is given by

$$G_\Phi = \frac{\partial \Phi_1}{\partial \Phi_2} = \frac{M_2}{M_{dyn1} + R_b/V_\Phi}, \tag{2.12}$$

where $M_{dyn} = R_{dyn1}/V_\Phi$ is the intrinsic current sensitivity of the sensor SQUID. The flux gain should be sufficiently high, so the amplified flux noise of the sensor SQUID is larger than the noise contributions of the second stage and the room temperature readout electronics. Hence, in a well-designed two-stage SQUID system, the overall system noise is determined by the sensor SQUID.

Another problem it that since the flux-to-voltage characteristic of the SQUID is periodic, we can only operate the amplifier in a small dynamic range around the

steepest part of $V - \Phi$ curve where the voltage response is almost linear. For a dc SQUID the linear range is taken as $\frac{1}{4}\Phi_0$ [45]. By introducing the second stage SQUID we have further reduced the dynamic range of the amplifier by a factor of G_Φ. This limitation can be overcome by using a SQUID amplifier with a negative feedback (a flux locked loop). The voltage signal from the SQUID is amplified, integrated and sent to a feedback coil, coupled to the SQUID loop. A feedback resistor R_{fb} is used to convert the voltage at the output of the integrator to the current in the feedback coil. As a result the total flux through the SQUID $\Phi_1 + \Phi_{fb}$ is constant. By adjusting the bias voltage V_b we can change the dc flux in the feedback loop and tune the working point of the SQUID.

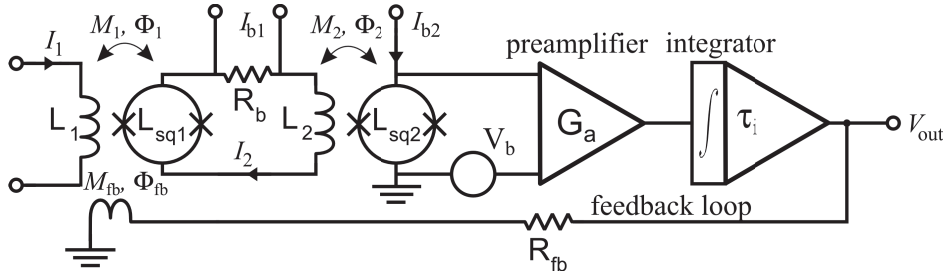

Figure 2.4**:** Scheme of 2-stage SQUID amplifier with a flux-locked loop circuit.

The voltage signal V_{out} at the output of the electronics is related to the signal flux as

$$V_{out} = \frac{G(\omega)}{1 + G(\omega)} \frac{R_{fb}}{M_{fb}} \Phi_1, \tag{2.13}$$

where $G(\omega)$ is called the open loop gain. For 2-stage SQUID it is

$$G(\omega) = G_\Phi V_\Phi G_a(\omega) \frac{M_{fb}}{R_{fb}}. \tag{2.14}$$

Since the open loop gain is high but finite, the flux through the SQUID is not really constant, but also includes some error ac flux $\Phi_{err} = \Phi_1 - \Phi_{fb}$. If Φ_{err} exceeds the linear range, the flux locked loop unlocks. A maximal slew rate (a speed of a flux change) that does not lead to SQUID unlocking is given by [48]

$$\frac{\partial \Phi_{SIG}}{\partial t} = \frac{\partial V G_a M_{fb}}{\tau_i R_{fb}}. \tag{2.15}$$

Preamplifier and automatic FLL reset circuit

Even after the room temperature electronics, the flux gain of the SQUID is in the order of $V_\Phi = 0.1 - 1\, V/\Phi_0$. Given that the SQUID noise spectral density at mK

temperatures $S_V < 1\,\mu\Phi 0/\sqrt{Hz}$, the voltage noise spectral density at the output of the SQUID electronics can be well below $1\,\mu V/\sqrt{Hz}$. Typical commercial ADC converters, like the one used for MiniGRAIL, have an input noise spectral density of $\sim 100nV/\sqrt{Hz}$, comparable with the signal from the SQUID. To eliminate the contribution of the converter noise we use a custom made 8-channel low-noise preamplifier with a fixed gain $G = 21$ and bandwidth $f_{-3dB} \approx 250$ kHz (figure 2.5(a)). We have measured the input noise of $\leq 6\,nV/\sqrt{Hz}$ for each preamp channel which is low enough not to introduce any noticeable extra noise in acquired data.

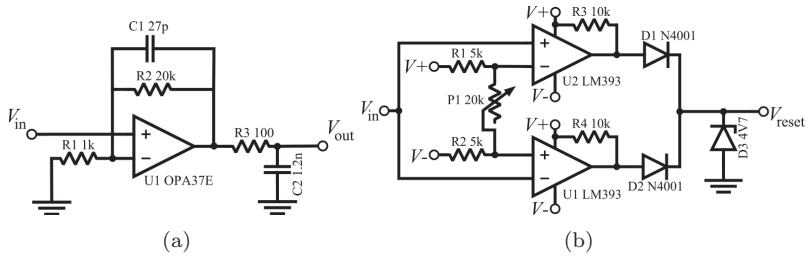

Figure 2.5**:** Preamplifier (a) and SQUID electronics reset (b) circuits.

If the flux locked loop is working properly (SQUID is locked) the integrator in the feedback loop keeps the SQUID at zero flux, so the DC level at SQUID electronics output is close to zero. If the FLL fails, the negative feedback does not compensate the signal flux in the SQUID anymore and the integrator quickly saturates resulting in a high voltage signal at the output of the electronics. Often it is enough to reset the integrator to restore the FLL operation. The SQUID electronics we are using [42] is not able to detect the overload condition and do a self reset, but it has an external TTL reset input for each channel.

We have developed a simple circuit (figure 2.5(b)) which monitors the output voltage of the SQUID electronics(V_{in} on the schematics) and if its absolute value exceeds a threshold voltage (set by $P1$) the comparators $U1$ and $U2$ should set V_{reset} output to high level. Because a Zener diode $D3$ limits the output voltage to TTL compatible level, the supply voltage can vary in a range of $5 - 15$ V.

Digitizing the acquired data

Because the ADC input is an analog signal with an infinite number of possible states, and the output is a digital discrete signal, the digitized data is distorted compared to the measured analog signal. This error is called quantization noise and limits the maximal signal to noise ratio (SNR) of an ADC converter. For N-bit ADC the expression for SNR is well known [49]

$$SNR = 6.02N + 1.76\,dB. \tag{2.16}$$

The quantization noise is uniformly spread in the spectra up to the Nyquist frequency $f_{sampl}/2$. So there are two obvious ways to increase the SNR - increasing the resolution or increasing the sampling frequency. From eq. 2.16 we note that a factor of 4 oversampling is equivalent to increase of ADC resolution by only one bit, so the oversampling by itself is not very efficient technique. However there is a class of ADC converters which offers high resolution and SNR by using a low cost low resolution ADC and a smart oversampling technique - the sigma-delta converters [49]. The high oversampling rate of such converters comes at the cost of low sampling rate(typically in order of $100 - 200\,kS/s$), but for digitizing wide dynamic range low bandwidth signals, like MiniGRAIL acquisition data, the sigma-delta converters seems to be an ideal solution.

Sigma-delta ADCs have a number of unique features:

- Oversampling: Sampling the input signal at a frequency that is much higher then the Nyquist frequency simplifies the acquisition chain, because there is no need for using low pass filters on each channel to suppress aliasing. It also distributes the quantization noise over a higher bandwidth, improving the signal to noise ratio.

- Noise shaping: Noise shaping filter acts as a low-pass filter to the input signal and a high-pass filter to the quantization noise. Thus, most of the quantization noise is pushed into higher frequencies which are filtered out at the output thus improving the SNR.

- Digital filtering: Integrated digital filters are used to attenuate the signal outside the band of interest.

- Decimation filtering: The output of the sigma-delta converter is a 1-bit data stream at the oversampling rate. The purpose of the decimation filter is to extract information from this data stream and reduce the data rate to a more useful value.

For MiniGRAIL we use 8 channel 24 bit NI 4472-PCI Sigma Delta ADC available from National Instruments. The disadvantage of this particular ADC card is that it has no external clock input, so it is clocked by less accurate PC clock generator. To overcome this problem we acquire the signal from a stable GPS clock system and do the timing afterwards in software.

The digitized data is saved in a file together with a header, which provides the information about timing, acquisition and system parameters. The header is written in a plain text as *Parameter Name: Value* pair. The ADC data is converted to voltage and saved in a 32 bit floating point format. The file structure is shown on figure 2.6.

Storage system

A NAS system used to store MiniGRAIL data is a 64-bit Linux PC with a 4 TB RAID5 attached to it. RAID system consists of 12 400 GB hard disks. 10 of them are

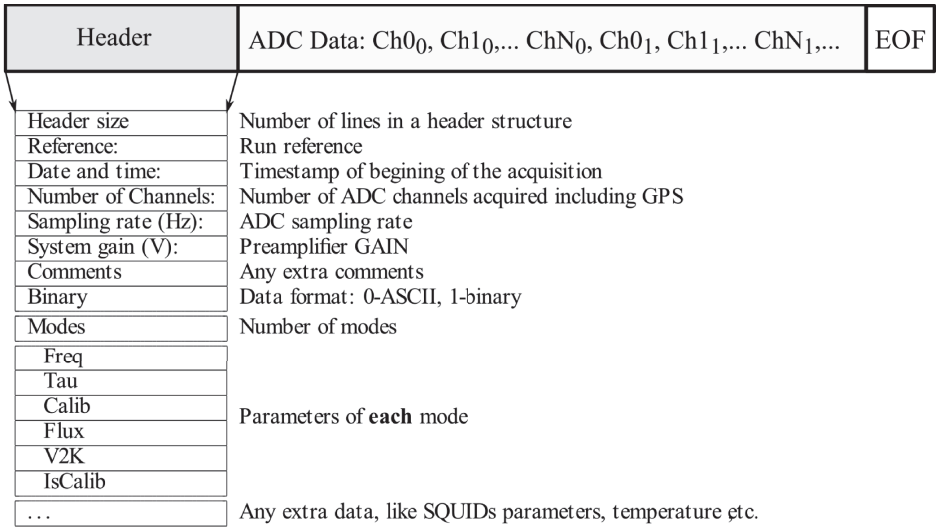

Figure 2.6**:** MiniGRAIL data acquisition file structure

used to store the data and 2 are reserved for redundancy, resulting in a total storage capacity of 4TB. With constantly growing hard disk capacity and decreasing price the size of the array can be tripled for a total price of less than 1000 euros.

2.1.2 Software

The acquisition software consists of two modules. The acquisition module communicates with the hardware (acquisition card, GPS,data storage systems) and the second module provides user interface functionality, allowing to set the acquisition settings and view current system parameters.

Acquisition module

The acquisition module is written in C/C++ using National Instruments NI-DAQ libraries to communicate with the acquisition card and "NMEA 0183" protocol to read data from GPS receiver.

The acquisition is done using double buffering technique to protect data integrity - the data is stored in memory in a circular buffer, which is divided in two halves. The hardware is writing data in one half of the buffer while the software reads it from the other half. This technique introduces a delay in acquisition equal to $\Delta\tau_{acq} = L_{buf}/2f_{sampl}$, where L_{buf} is the size of a circular buffer in samples. But since all current MiniGRAIL data analysis routines are offline, this time delay is not an issue. The driver monitors the integrity of the buffer and generates an event on error. The

software handles this events and can restart the acquisition if an unrecoverable error occurs.

Since the acquisition system does not support external frequency generator input and the internal PC clock generator might not be accurate enough - one of the acquisition channels is always connected to GPS system PPS (Pulse Per Second) signal output. This is a high precision timed delta-like signal generated every second by GPS hardware.

When the acquisition is started it is initialized as follows:

1. Reading acquisition settings from use interface (UI) module
2. Initializing ADC card. Set buffer size, acquisition frequency, time, etc.
3. Get time stamp from GPS clock.
4. Start acquisition.
5. If data in the acquisition buffer is ready, read it.
6. Find the first PPS signal and start saving the data after that point
7. Correct the acquisition timing to account the skipped data

By using PPS as a trigger, the time of the acquisition start is defined and the timing of any data sample can be calculated from it. This is very important for later data analysis. In step 4 there is always a delay between the software command to start the acquisition and the hardware response. It depends a lot on the operation system and is not constant. It is possible to estimate it by measuring the time difference between just before the step 4 and after step 5.By subtracting the length of acquired data we can calculate the initialization delay. The measured value was stable around $150\,ms$ when the computer was only busy running the acquisition, but was very unstable, sometimes reaching more then one second delay, when the PC was under stress load.

Thus, we can state the delay to be always much less than one second, in normal operating conditions, so it is enough to discard the data before the second PPS signal and increase the time stamp, received from GPS by 1 second.

UI module

The user interface module is written in C# and provides a user friendly way to set acquisition parameters and current system properties. It allows to set the following acquisition parameters:

- Acquisition frequency.
- Acquisition buffer size.
- Acquisition time for one file
- Total acquisition time or continuous mode.

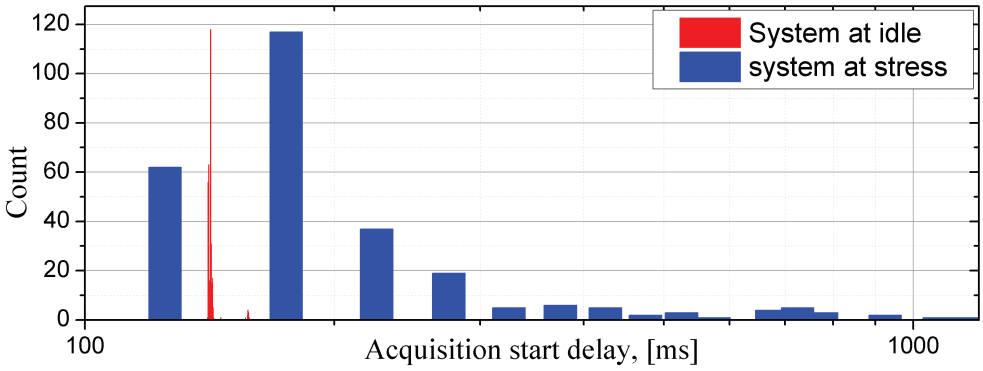

Figure 2.7**:** Acquisition initialization delay for PC running only acquisition and under stress testing

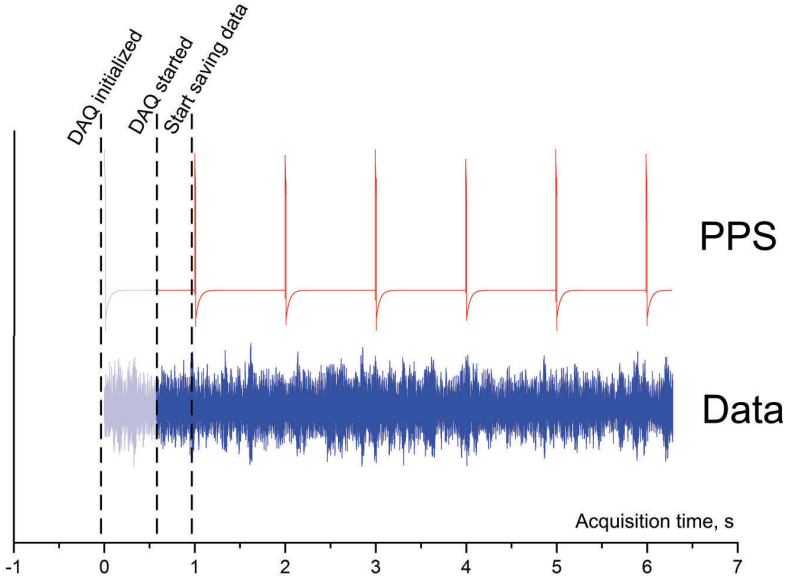

Figure 2.8**:** Acquisition system delay elimination

- Properties of the visible modes: frequency, quality factor, calibration constants.
- Properties of the read-out chain: SQUID parameters, preamp gain.

Module also displays the acquisition and error logs. The software also reacts to the error events generated by the ADC driver and can reinitialize the system and restart the acquisition.

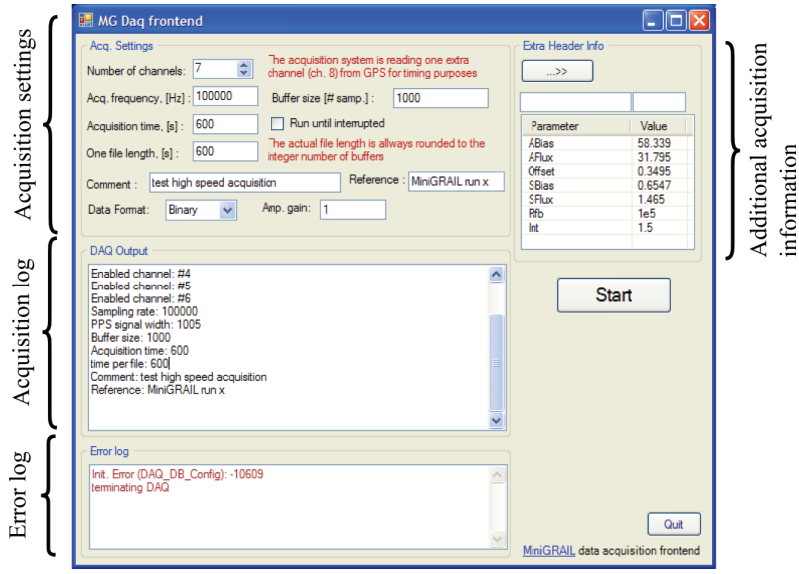

Figure 2.9**:** DAQ front end user interface

2.2 Data preprocessing

The data processing software is used to prepare the raw acquired data for data analysis. It can perform the following tasks:

- Filter out bad data. The filtering script scans through the acquisition files and calculates signal to noise ratio (SNR) of the resonant modes. If the SNR is below a certain threshold then the file is marked as bad data and not used in further data processing procedures.

- Calculate the precise acquisition frequency. Saving GPS PPS signal together with the MiniGRAIL data allows to calculate the accurate value of the acquisition frequency.

- Do decimation to reduce a data stream. To reduce the data processing time only the data in the band of interest can be extracted from the raw data set. For acquisition system sampling frequency of 18.6 KHz,according to Nyquist-Shannon sampling theorem the signal with frequencies up to 9.3 kHz can be reconstructed. But most of the time we are only interested in a few hundred Hz band around 3 kHz, where all the normal modes are located.

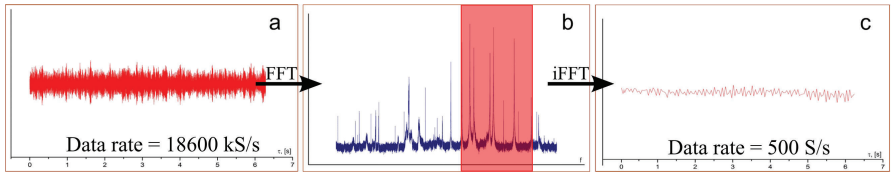

Figure 2.10**:** Data subsampling

2.3 Data transfer

Once available, the data from MiniGRAIL will be transferred to Theoretical Physics Department of University of Geneva for data analysis. The transfer algorithm and data analysis pipeline developed in Geneva is described in [31]. The acquired MiniGRAIL data is first copied from the acquisition PC to "To_transfer" folder on the NAS. Once the data is transferred it is moved to "Transferred" folder, so it is never deleted from MiniGRAIL storage. The transfer is done with command line shell script calling *rsync* utility [50]. We have measured an average transfer rate of $4.5\,MB/s$, which is much higher than the acquisition data rate of $600\,kB/s$.